

Moment-based Kalman Filter design for cell population balance models in batch fermentation processes ^{*}

P. Jerono ^{*} A. Schaum ^{*} T. Meurer ^{*}

^{*} *Chair of Automatic Control, Faculty of Engineering, Kiel University, Kiel, Germany, {pj,alsc,tm}@tf.uni-kiel.de*

Abstract: The observer design problem for the cell population estimation in a yeast batch process is addressed. The cell population balance model is described by a partial integro-differential equation coupled with a set of ordinary differential equations. Based on the observability property of the first moment of the cell distribution and the structural observability of the discretized cell population balance model, an extended Kalman Filter operating on on-line biomass measurements is designed for the model equations. The observer is validated using experimental data.

Keywords: Cell population balance models, partial integro-differential equation, yeast fermentation, process control, Kalman filtering, moments of a distribution.

1. INTRODUCTION

Observers are a key component of on-line monitoring when on-line sensors are not available, do not have an adequate accuracy or are associated with high cost. The basis of an observer is given by the underlying model (or digital twin) which is typically designed to capture key characteristics of the process.

In bioprocess technology the models of bioreactors are divided into different levels of detail. The classification is usually based on (un-)structured and (un-)segregated models [Schügerl and Bellgard 2000]. Unstructured models do not describe the microorganism in detail and assume that one type of biomass is equally distributed in the reactor, whereas in structured models different types of biomass are considered. Segregated models do also take into account the distributed and statistical nature of the biological process by means of cell mass, size or age. Segregated models like the cell population balance model are typically described by a partial integro-differential equation [Tsuchiya et al. 1966, Villadsen 1999, Mhaskar et al. 2002, Daoutidis and Henson 2002]. Cell population balance models provide a more detailed description of the species in a biological reactor compared to classical mass balance models. As a trade off, the parameterization and identification of cell population balance models is more complex and requires suitable measurement data revealing insight to the cell distribution. For this purpose cell distribution measurements are usually obtained by special designed experiments in a small scale or by time consuming off-line analysis [Waldherr 2018]. This motivates to design an observer driven by classical available on-line measurement data, like optical density measurements, for the estimation of the cell distribution in a biological growth process.

The observer design problem for (un-)structured and un-segregated bioreactor models has been addressed by different authors considering high-gain observers [Gauthier et al. 1992], asymptotic observers [Dochain et al. 1992, Dochain 2003], dissipativity-based observers [Moreno 2005, Schaum and Moreno 2006.], Kalman Filters [Dewasme et al. 2013], and interval observers [Moisan et al. 2009, Goffaux et al. 2009]. The observer design problem for segregated cell population balance models in bioreactors is addressed in [Schaum and Jerono 2019], where a moment-based observer for a reactor in chemostat operation is designed. Cell population balance models are mathematically close to the models of crystallization processes. In this area Luenberger observers, high-gain observers and Kalman Filters [Motz et al. 2008, Bakir et al. 2006, Mesbah et al. 2011] have been designed based on finite-dimensional and moment-based model approximations.

In the present work an extended Kalman Filter for the estimation of the cell mass distribution and the glucose concentration based on on-line biomass measurements by means of the optical density in a yeast fermentation process is designed in an early lumping approach. For proof of concept the yeast fermentation is carried out under anaerobic conditions, so that the reactions can be described taking into account only biomass, substrate and by-product concentrations.

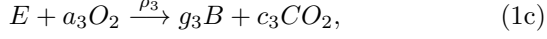
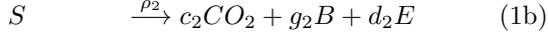
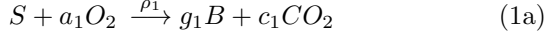
The paper is organized as follows. In Section 2 the mathematical model of yeast growth is presented. In Section 3 the model equations are discretized. In Section 4 observability properties are established and the observer is designed for the discretized model equations. The experimental setup of the yeast fermentation is presented and the measurements are described in Section 5. In Section 6 the designed observer is validated using the experimental data. In Section 7 conclusions are drawn.

^{*} Funded by the Deutsche Forschungsgemeinschaft (DFG, German Research Foundation) – Project-ID 395461267.

2. MODEL DESCRIPTION

$$B(q) = \frac{2\Gamma_f(q)}{\Gamma_f(2q)}.$$

Yeast growth follows the three substantial pathways



where B , S , E , O_2 and CO_2 denote the biomass, glucose, ethanol, oxygen, and carbon dioxide compounds respectively. The reaction rates are denoted by ρ_i and the related stoichiometric coefficients are given by a_i , g_i and d_i , where $i \in \{1, 2, 3\}$. Reaction (1a) describes the oxidation of glucose to biomass, reaction (1b) the anaerobic production of ethanol and biomass and reaction (1c) describes the oxidation of ethanol to biomass. Usually the reaction rates ρ_i are chosen to capture characteristic effects of yeast growth like the crab-tree effect [Deken 1966]. When considering anaerobic growth of yeast only reaction (1b) takes place and the reaction dynamics can be described by a Monod growth rate

$$\rho(s) = k_s \frac{s}{s + K_s}, \quad (2)$$

where k_s is the maximum growth, K_s is the half saturation constant and s denotes the glucose concentration. Based on the reaction scheme for anaerobic yeast growth in a batch reactor the following set of ordinary differential equations for the mass balance can be derived

$$\dot{b} = g_2 \rho(s) b, \quad b(0) = b_0 \quad (3a)$$

$$\dot{s} = -\rho(s) b, \quad s(0) = s_0 \quad (3b)$$

$$\dot{e} = d_2 \rho(s) b, \quad e(0) = e_0, \quad (3c)$$

where b , s and e denote the concentrations of biomass, glucose and ethanol, respectively.

The mass balance is complemented by the general cell population balance model [Villadsen 1999, Mhaskar et al. 2002, Daoutidis and Henson 2002, Mantzaris and Daoutidis 2004] in batch operation mode

$$\begin{aligned} \partial_t n(m, t) = & -g_2 \partial_m [r(m, s) n(m, t)] + \\ & -\Gamma(m, s) n(m, t) + \\ & + 2 \int_m^{m_*} \Gamma(\mu, s) p(m, \mu) n(\mu, t) d\mu \end{aligned} \quad (4a)$$

$$\dot{s}(t) = - \int_0^{m_*} r(m, s) n(m, t) dm \quad (4b)$$

$$n(m_*, t) = 0 \quad (4c)$$

$$n(m, 0) = n_0(m), \quad s(0) = s_0, \quad (4d)$$

with $m \in [0, m_*]$ being the cell mass, m_* the maximum cell mass, $n(m, t)$ the cell density of mass m at time t , r the cell growth rate function, Γ the cell division rate, p the partition probability density function, i.e., $p(m, \mu)$ is the probability that by division of a cell of mass μ a cell of mass m is produced. Note that in virtue of its definition, p has the property that

$$\forall \mu \leq m : \quad p(m, \mu) = 0 \quad (5)$$

and is chosen as a symmetric binomial distribution [Mantzaris and Daoutidis 2004]

$$p(m, \mu) = \frac{1}{B(q)} \frac{1}{\mu} \left(\frac{m}{\mu} \right)^{q-1} \left(1 - \frac{m}{\mu} \right)^{q-1},$$

with the normalization factor

In the sequel a linear dependency of r on the cell mass m , as discussed in [Mantzaris and Daoutidis 2004], is considered so that

$$r(m, s) = \rho(s) m. \quad (6)$$

Moreover the division rate $\Gamma(m, s)$ is assumed to be proportional to the cell growth rate

$$\Gamma(m, s) = \gamma(m) r(m, s). \quad (7)$$

The function $\gamma(m)$ is chosen to be a ramp function

$$\gamma(m) = \begin{cases} 0, & \text{if } m \leq m^* \\ \beta m, & \text{if } m^* < m, \end{cases} \quad (8)$$

where the minimal cell mass required for division is given by m^* and β is a constant. Note that the existence, uniqueness and positivity of solutions in $L^1 \times \mathbb{R}_+$ for (4) has been shown in [Benich et al. 2018]. Taking the first moment of the cell population balance model

$$b(t) = \int_0^{m_*} m n(m, t) dm \quad (9)$$

its time derivative results in

$$\dot{b}(t) = \int_0^{m_*} m \partial_t n(m, t) dm. \quad (10)$$

Recalling mass conservation during cell division [Mantzaris and Daoutidis 2004, Schaum and Jerono 2019], one obtains

$$\begin{aligned} \dot{b}(t) = g_2 \rho(s) \int_0^{m_*} m n(m, t) dm = g_2 \rho(s) b \\ \dot{s}(t) = -\rho(s) \int_0^{m_*} m n(m, t) dm = -\rho(s) b, \end{aligned} \quad (11)$$

which corresponds to the mass balance model (3a) and (3b). In an analogous manner the dynamics of product formation can be included into (4).

3. DISCRETIZED MODEL EQUATIONS

In order to design an observer in the framework of an early lumping approach, the cell population partial integro-differential equation (4) needs to be discretized in the mass domain. Here the partial derivative is approximated using a backwards finite differences scheme with step size Δm . For the approximation of the integral term the trapezoidal rule is chosen. The discretized model equations then read

$$\begin{aligned} \dot{n}_i = & -\frac{1}{\Delta m} g_2 \rho(s) m_i (n_i - n_{i-1}) - \Gamma(m_i, s) n_i + \\ & + 2 \Delta m \sum_{j=i}^z (\Gamma(m_j, s) p(m_i, m_j) n_j + \\ & + \Gamma(m_{j+1}, s) p(m_i, m_{j+1}) n_{j+1}) \end{aligned} \quad (12a)$$

$$\dot{s} = -\rho(s) b \quad (12b)$$

$$\dot{e} = d_2 \rho(s) b \quad (12c)$$

$$n(m_{z+1}, t) = 0 \quad (12d)$$

$$n(m, 0) = n_0(m), \quad s(0) = s_0, \quad e(0) = e_0.$$

By introducing the state vector $\mathbf{x} = [n_1, \dots, n_z, s, e]^T$ with z denoting the number of interior discretization points, (12) can be re-cast into the form

$$\dot{\mathbf{x}} = \mathbf{f}(\mathbf{x}) = \begin{bmatrix} f_{n,1}(\mathbf{x}) \\ \vdots \\ f_{n,z}(\mathbf{x}) \\ f_s(\mathbf{x}) \\ f_e(\mathbf{x}) \end{bmatrix}, \quad \mathbf{x}(0) = \mathbf{x}_0 \in \mathbb{R}^{z+2}. \quad (13)$$

Note that the boundaries of the cell distribution $n(0, t)$ and $n(m_*, t)$ can be excluded from the state vector, because $\rho(s)m_{\min} = 0$ and $n(m_*, t) = 0$. The measurement equation of biomass b using the trapezoidal rule reads

$$y = h(\mathbf{x}) = b = \Delta m \sum_{i=1}^z m_i n_i. \quad (14)$$

4. OBSERVER DESIGN

4.1 Observability properties of the moment model

The observability properties of (3a), (3b) when measuring the biomass concentration $y = b$ for the class of reactor models (11) has been discussed in the literature [Schaum et al. 2005, 2007, Moreno and Dochain 2005] revealing the detectability property for non monotonic growth rates $\rho(s)$ and global observability in $\mathbb{R}_{\geq 0}$ for monotonic growth rates. Based on these results the convergence of the observer error in the first moment of the cell distribution can also be concluded [Schaum and Jerono 2019]. Note that the observability property of the system (3) only holds when the product formation, i.e., the ethanol production (3c) is not taken into account. Since for anaerobic yeast growth ethanol will only be produced and not consumed, i.e., there is no coupling of the ethanol concentration into the biomass or glucose dynamics, the ethanol dynamics can simply be neglected in the state vector. Nevertheless since the initial ethanol concentration in a yeast batch experiment is usually known, in the observer design the ethanol dynamics can be estimated by the simulator using the estimated biomass [Rapaport and Dochain 2020].

4.2 Observability of the cell population balance model

The observability of the cell distribution estimation for the discretized model (neglecting the product formation (12c) as outlined before) is analyzed subsequently. For this purpose the graph-theoretical approach to analyse structural observability is followed [Chan and Shachter 1992, Liu et al. 2013]. The basic idea is to map the interconnection between the system vector field $\mathbf{f}(\mathbf{x})$ and the states \mathbf{x} into a network graph, where an interconnection from x_i to x_j is given when $\frac{\partial f_i(\mathbf{x})}{\partial x_j} \neq 0$. This network is then analyzed to identify the nodes which have to be measured to achieve structural observability, i.e., the corresponding observability map of the system

$$\mathcal{O} = \frac{\partial}{\partial \mathbf{x}} \begin{bmatrix} h(\mathbf{x}) \\ L_f^1 h(\mathbf{x}) \\ \vdots \\ L_f^{n-1} h(\mathbf{x}) \end{bmatrix} \quad (15)$$

has full rank considering that no linear dependencies occur due to unfavourable system parameters. Since the measurement equation (14) is not part of the system vector

field, for the analysis, the system equations are extended by the measurement $y = b$, i.e.,

$$\mathbf{f}_b(\mathbf{x}_b) = \begin{bmatrix} \mathbf{f}_n(\mathbf{x}_b) \\ f_s(\mathbf{x}_b) \\ \Delta m \sum_{i=1}^z m_i f_{n,i}(\mathbf{x}_b) \end{bmatrix}, \quad \mathbf{x}_b = \begin{bmatrix} n_1 \\ \vdots \\ n_z \\ s \\ b \end{bmatrix}. \quad (16)$$

Taking into account (12a), (12b), (14) and (16) the so-called inference diagram shown in Figure 1 is obtained.

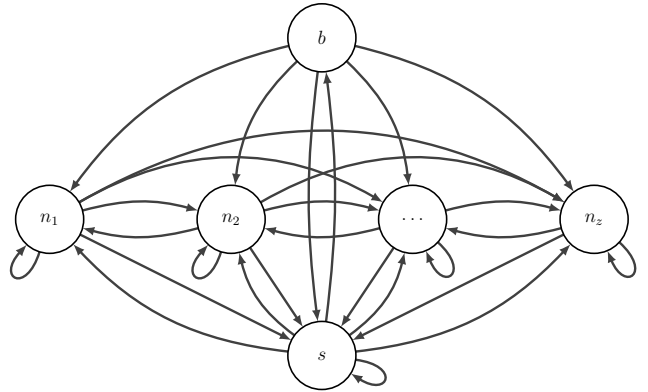


Fig. 1. Inference diagram of the system equations (16).

In the next step the network is structured into strongly connected components, i.e., vertexes including nodes such that every vertex is reachable from another vertex. In case of Figure 1 it can be seen that every node is a strongly connected component. For n_1, \dots, n_z this is mainly given due to the cell growth and birth term in equation (12a). Next, the nodes which have no incoming connection need to be identified. These nodes need to be measured in order to achieve structural observability. It can be seen that every node in Figure 1 has at least one incoming connection. This reveals that structural observability is achieved when one arbitrary node of the network is measured. Thus the structural observability of the system for $y = b$ can be concluded. Since all nodes are strongly connected components regardless of the number of discretization points z , this result holds for any $z \in \mathbb{N}_{\geq 2}$. Note that b is the only node having one incoming interconnection, namely from s to b . When the analysis is carried out for substrate independent growth rates, it becomes directly clear that in this scenario the measurement equation $y = b$ is the only configuration ensuring structural observability with respect to the cell distribution. It has to be pointed out that structural observability is lost when $\rho(s) = 0$. Therefore convergence of the observer error has to be ensured before the end of the batch experiment.

4.3 Extended Kalman Filter design

For practical applications the Kalman Filter is a well established observer scheme. The Kalman Filter is a statistical optimal observer which minimizes the covariance of the estimation error and is well suited for noisy measurements [Gelb 1978]. Compared to the growth dynamics of yeast in a batch reactor the measurement sample frequency is relatively high, so that the extended Kalman Filter is designed

within a continuous update scheme [Gelb 1978, Lewis et al. 2017]. The corresponding early lumping extended Kalman Filter to be implemented hence reads

$$\dot{\hat{n}}_i = f_{n,i}(\hat{\mathbf{x}}) + l_i(y - \hat{b}) + \omega_i, \quad i = 1, 2, \dots, z \quad (17a)$$

$$\dot{\hat{s}} = f_s(\hat{\mathbf{x}}) + l_s(y - \hat{b}) + \omega_s \quad (17b)$$

$$\dot{\hat{e}} = f_e(\hat{\mathbf{x}}) \quad (17c)$$

$$\dot{P} = FP + PF^T + Q - PH^T R^{-1} HP \quad (17d)$$

$$\mathbf{l} = PH^T R^{-1} \quad (17e)$$

$$\hat{n}(m_{z+1}, t) = 0 \quad (17f)$$

$$\hat{n}(m, 0) = n_0(m), \quad s(0) = s_0, \quad e(0) = e_0$$

$$\hat{b} = h(\hat{\mathbf{x}}) = \Delta m \sum_{i=1}^z m_i \hat{n}_i \quad (17g)$$

$$y = b + v = \int_0^{m^*} m n(m, t) dm + v, \quad (17h)$$

where $\mathbf{l} = [l_1, \dots, l_z, l_s]$ is the correction gain vector, $\omega_i \sim \mathcal{N}(0, Q_i)$, $i \in \{1, \dots, z\}$, $\omega_s \sim \mathcal{N}(0, Q_s)$ and $v \sim \mathcal{N}(0, R)$ are assumed to be gaussian distributed and the state vector is given by $\hat{\mathbf{x}} = [\hat{n}_1, \dots, \hat{n}_z, \hat{s}]^T$. The associated Jacobians in the Kalman Filter equations (17d) and (17e) read

$$F = \begin{bmatrix} \frac{\partial \dot{\hat{n}}_1}{\partial n_1} & \dots & \frac{\partial \dot{\hat{n}}_1}{\partial n_z} & \frac{\partial \dot{\hat{n}}_1}{\partial s} \\ \vdots & \ddots & \vdots & \vdots \\ \frac{\partial \dot{\hat{n}}_z}{\partial n_1} & \dots & \frac{\partial \dot{\hat{n}}_z}{\partial n_z} & \frac{\partial \dot{\hat{n}}_z}{\partial s} \\ \frac{\partial \dot{\hat{s}}}{\partial n_1} & \dots & \frac{\partial \dot{\hat{s}}}{\partial n_z} & \frac{\partial \dot{\hat{s}}}{\partial s} \\ \frac{\partial \hat{b}}{\partial n_1} & \dots & \frac{\partial \hat{b}}{\partial n_z} & \frac{\partial \hat{b}}{\partial s} \end{bmatrix} \quad (18a)$$

$$H = [\Delta m m_1, \dots, \Delta m m_z, 0]. \quad (18b)$$

Note that in (17c) \hat{e} is only driven by the simulator and thus is not included in the state vector.

5. EXPERIMENTAL SETUP

A batch yeast fermentation experiment was carried out in a 2 liter stirred-tank reactor. The process conditions are listed in Table 1. To ensure that the yeast growth process is performed under anaerobic conditions, the reactor is aerated with nitrogen. Optical density measurements are taken on-line at 600 nm wavelength. Glucose and ethanol measurements are evaluated off-line at discrete time instances. The parameters of the mass balance model (3), namely k_s , K_s , b_2 and d_2 have been adapted to fit the experimental data from previous experiments. In the identification process the biomass growth rate $\rho(s)$ remains almost constant for glucose concentrations $s \gg K_s$ and ethanol concentrations $e > 0$, so that inhibition of the growth rate by ethanol formation has no measurable impact for the considered experimental setup and is therefore neglected in the model description. The parameters of the cell population balance model with respect to cell division and birth have been identified with $z = 51$ by taking the presented measurement data (see Figure 3) into account. The complete set of model parameters is listed in Table 2.

Table 1. Process conditions

Parameter	Value	Unit
Temperatur	25	°C
Aeration (N ₂)	0.10	vvm
controlled pH	5.5	-
Stirrer speed	750	rpm
Glucose (s_0)	8.496	g/l

Table 2. Model parameter

Parameter	Value	Unit
k_s	2.9660	h ⁻¹
K_s	0.7000	gS/l
g_2	0.1810	gB/gS
d_2	0.4503	gE/gS
q	5.0000	-
m^*	$5.4808 \cdot 10^{-11}$	g
m_*	$1.5000 \cdot 10^{-10}$	g
β	$6.7083 \cdot 10^{21}$	-
γ_*	$5.4182 \cdot 10^{11}$	-
ϱ_n	$44.6801 \cdot 10^4$	g/l

5.1 Cell distribution measurements

The cell distribution in terms of number of cells with a specific diameter have been measured by the Casy TT cell counter and cell analyzer from Omni Life Science (OLS). Since the considered cell population balance model is constructed for cell density functions with respect to mass, the raw measurements of the cell analyzer have been transformed to the mass domain. The mass density per volume of a cell, namely ϱ_n , for this transformation was chosen such that the first moment of the cell distribution fits the biomass dry weight measurements of the related probe. The value of ϱ_n is also listed in Table 2. In order to determine the cell distribution density function the inverse function of the trapezoidal integration formula

$$n(m_{i+1}, t) = \frac{2}{m_{i+1} - m_i} \int_{m_i}^{m_{i+1}} n(m, t) dm - n(m_i, t)$$

was applied to the filtered measurement, where the integral term is given by the measurement and $i \in \{1, \dots, 399\}$ being the number of measurement channels of the cell analyzer which are mapped to $z = 51$ by linear interpolation.

6. RESULTS

In Figure 2, 3 and 4 the results of the implemented extended Kalman Filter observer scheme are compared with an open-loop simulation, i.e., when no correction based on the biomass measurement is applied. The initial states of the observer and the open-loop simulation are chosen to be $\hat{\mathbf{x}} = [2.22 \cdot 10^{10} \sin^4(\pi m/m_*), 8.6]$ and the initial ethanol concentration is given by $\hat{e}(0) = 0.145$ g/l. The values of Q_i and $P_{0,i}$ are chosen to be shifted and left-side truncated gaussian functions, which goes along with the assumption that the discretized cell population balance model is more accurate at the edges of the mass domain. Figure 2 shows the estimation of the biomass, glucose and ethanol trajectories. The discrete snapshots of the cell population distribution estimation are shown in Figure 3. The estimated states of the Kalman Filter are given by the solid red lines. The open-loop simulation is represented by the dashed green lines and the measurements are given by the

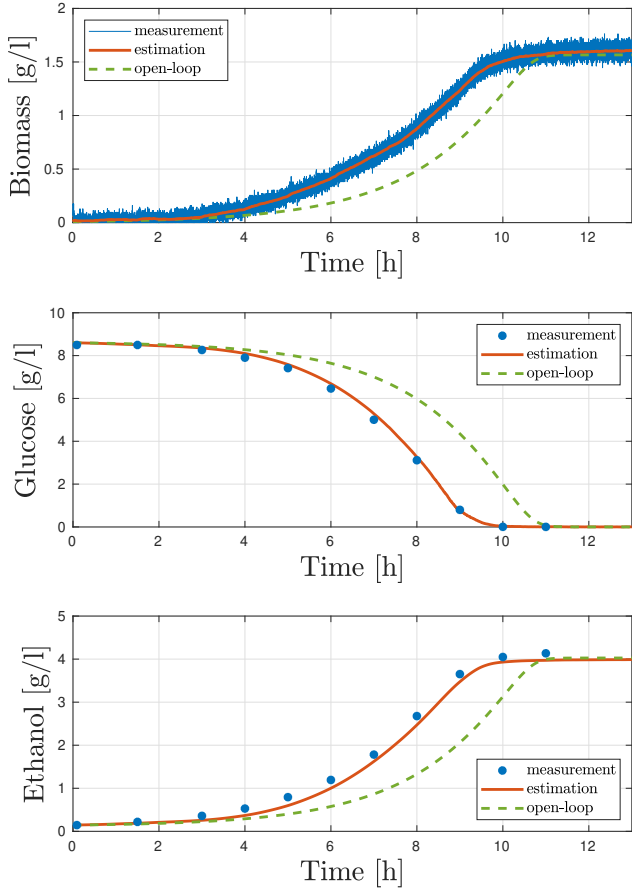


Fig. 2. Estimation of the biomass, glucose and ethanol concentration (solid red), open-loop simulation (dashed green) and measurements (solid blue and blue markers).

solid blue lines and blue markers. Note that the glucose, ethanol, and cell distribution measurements are obtained off-line and are only used for validation purpose since the observer operates only on on-line biomass measurements. The estimation of the ethanol concentration is only driven by the simulator due to the lack of observability, i.e., in the estimation of the ethanol concentration a correction term is not applied. Figure 4 shows the comparison of the estimation error in the cell distribution ϵ_1 given by

$$\epsilon_1(t) = \frac{1}{\int_0^{m_*} n(m, t) dm} \int_0^{m_*} |n(m, t) - \hat{n}(m, t)| dm$$

and corresponds to a normalized L^1 -norm which is approximated by the trapezoidal rule and evaluated at the discrete measurement time instances. The estimation error in the glucose concentration ϵ_2 is simply given by

$$\epsilon_2(t) = |s(t) - \hat{s}(t)|.$$

Note that for batch experiments the initial estimation errors of the concentrations is relative low because the initial concentrations are part of the process conditions which are usually known. Nevertheless it can be seen that during the experiment the open-loop simulation has significant errors compared to the measurements of biomass, glucose, ethanol, and the cell population distribution. At the end of the batch experiment these errors become small again because of the relative low initial error in the glucose component and the known stoichiometric coefficients of the

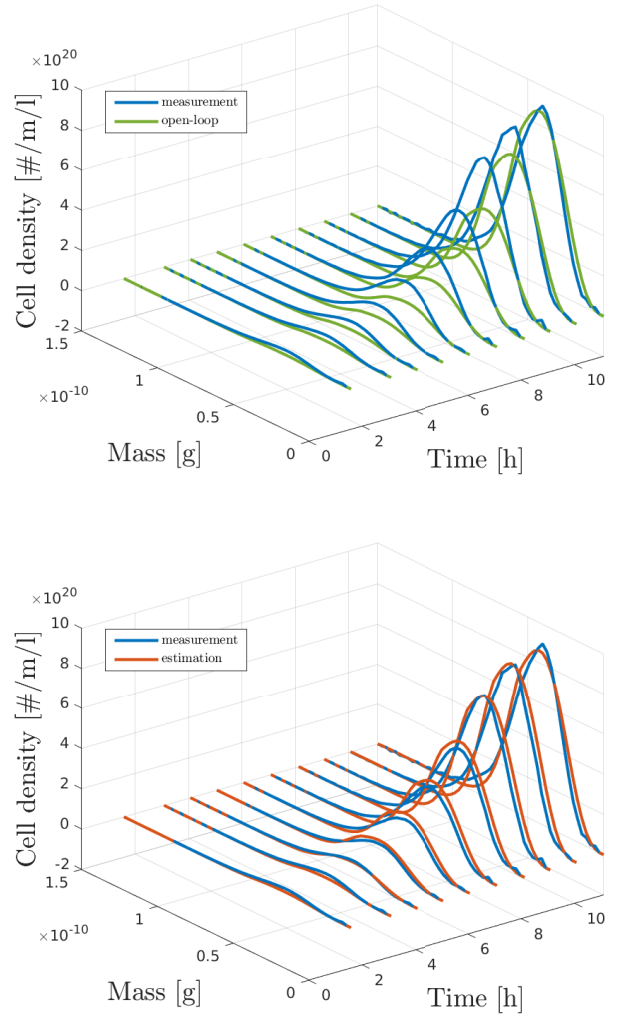


Fig. 3. Snapshots of the cell population distribution estimation (solid red), open-loop simulation (dashed green) and measurements (solid blue).

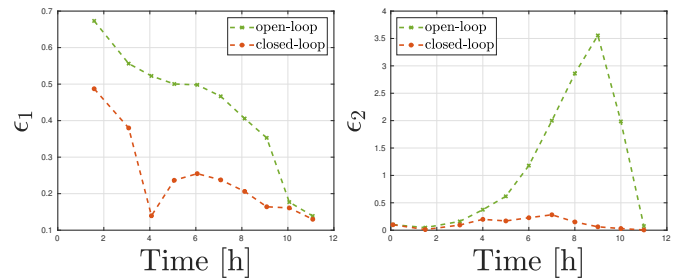


Fig. 4. Estimation error ϵ_1 and ϵ_2 of the extended Kalman Filter (red star markers) and the open-loop simulation (green cross markers).

model. Contrary, the proposed extended Kalman Filter has a good estimation performance over the whole experiment and has a fast convergence of the estimation error in the L^1 -norm of the cell distribution, namely ϵ_1 , shown in Figure 4. In addition the estimation of the ethanol concentration (equation (17c)) of the observer has a significant better performance compared to the open-loop simulation.

7. CONCLUSION

In this work the observer design problem for the cell population distribution in a yeast batch fermentation with continuous biomass measurements is addressed. The structural observability properties of the cell population balance model for biomass measurements are established and an extended Kalman Filter for the discretized model equations operating only on on-line biomass measurements is designed and validated in an experimental batch process. The extended Kalman Filter has a good performance in estimating the cell population distribution and glucose concentration, enabling on-line information of these state variables. Even though the observability of the system is not given when the product formation is taken into account, the estimation of the product concentration only driven by the simulator of the observer shows a significant better performance compared to the open-loop simulation.

REFERENCES

- Bakir, T., Othman, S., Fevotte, G., and Hammouri, G. (2006). Nonlinear observer of crystal-size distribution during batch crystallization. *AIChE Journal*, 52 (6), 2188–2197.
- Beniich, N., Abouzaid, B., and Dochain, D. (2018). On the existence and positivity of a mass structured cell population model. *Appl. Math. Sci.*, 12 (19), 921–934.
- Chan, B.Y. and Shachter, R.D. (1992). Structural Controllability and Observability in Influence Diagrams. *Proceedings of the 8th Conference on Uncertainty in Artificial Intelligence*, 25–32.
- Daoutidis, P. and Henson, M. (2002). Dynamics and control of cell populations in continuous bioreactors. *AIChE Symposium Series*, 326, 274–289.
- Deken, R.H.D. (1966). The Crabtree Effect: A Regulatory System in Yeast. *Microbiology*, 44(2), 149–156.
- Dewasme, L., Goffaux, G., Hantson, A.L., and Wouwer, A.V. (2013). Experimental validation of an Extended Kalman Filter estimating acetate concentration in *E. coli* cultures. *Journal of Process Control*, 23(2), 148–157.
- Dochain, D. (2003). State observers for processes with uncertain kinetics. *Int. J. Control*, 76 (15), 1483–1492.
- Dochain, D., Perrier, M., and Ydstie, B. (1992). Asymptotic observers for stirred tank reactors. *Chem. Eng. Sci.*, 47 (15/16), 4167–4177.
- Gauthier, J.P., Hammouri, H., and Othman, S. (1992). A simple observer for nonlinear systems: Applications to bioreactors. *IEEE Trans. Autom. Control.*, 37 (6), 875–880.
- Gelb, A. (1978). *Applied Optimal Estimation*. M.I.T. Press, Cambridge.
- Goffaux, G., Wouwer, A.V., and Bernard, O. (2009). Continuous - discrete interval observers for monitoring microalgae cultures. *Biotechnol. Progr.*, 25 (3), 667–675.
- Lewis, F., Xie, L., and Popa, D. (2017). *Optimal and Robust Estimation: With an Introduction to Stochastic Control Theory, Second Edition*. Automation and Control Engineering. CRC Press.
- Liu, Y.Y., Slotine, J.J., and Barabasi, A.L. (2013). Observability of complex systems. *Proceedings of the National Academy of Sciences of the United States of America*, 110(7), 2460–2465.
- Mantzaris, N.V. and Daoutidis, P. (2004). Cell population balance modeling and control in continuous bioreactors. *J. Process Control*, 14, 775–784.
- Mesbah, A., Huesman, A.E.M., Kramer, H.J.M., and den Hof, P.M.J.V. (2011). A comparison of nonlinear observers for output feedback model-based control of seeded batch crystallization processes. *J. Process Control*, 21 (4), 652–666.
- Mhaskar, P., Hjortso, M.A., and Henson, M. (2002). Cell population modeling and parameter estimation for continuous cultures of *saccharomyces cerevisiae*. *Biotechnol. Progr.*, 18, 1010–1026.
- Moisan, M., Bernard, O., and Gouze, J.L. (2009). Near optimal interval observers bundle for uncertain bioreactors. *Automatica*, 45, 291–295.
- Moreno, J.A. (2005). Approximate observer error linearization by dissipativity methods. In T. Meurer, K. Graichen, and E.D. Gilles (eds.), *Control and Observer Design for Nonlinear Finite and Infinite Dimensional Systems*, volume 322 of *Lecture Notes in Control and Information Sciences*, 35–51. Springer.
- Moreno, J.A. and Dochain, D. (2005). Global observability and detectability analysis of uncertain reaction systems. *16th IFAC World Congress*, 38(1), 37–42.
- Motz, S., Mannal, S., and Gilles, E.D. (2008). State estimation in batch crystallization using reduced population models. *J. Process Control*, 18 (3-4), 361–374.
- Rapaport, A. and Dochain, D. (2020). A robust asymptotic observer for systems that converge to unobservable states - A batch reactor case study. *IEEE Transactions on Automatic Control*, 65(6), 2693–2699.
- Schaum, A. and Jerono, P. (2019). Observability analysis and observer design for a class of cell population balance models. *IFAC-PapersOnLine*, 52(2), 189–194.
- Schaum, A., Moreno, J.A., Diaz-Salgado, J., and Alvarez, J. (2007). Dissipativity-based observer and feedback control design for a class of chemical reactors. In *Proceedings 8th International IFAC Symposium on Dynamics and Control of Process Systems*, 73–78.
- Schaum, A., Moreno, J.A., and Vargas, A. (2005). Global observability and detectability analysis for a class of nonlinear models of biological processes with bad inputs. *Proceedings of the 2nd IEEE Int. Conf. on Electrical and Electronics Engineering, (ICEEE) and XI Conf. on Electrical Engineering (CIE)*, 343–346.
- Schaum, A. and Moreno, J. (2006). Dissipativity based observer design for a class of biochemical process models. *2do. Congreso de Computacion, Informatica, Biomedica y Electronica (CONCIBE 2006), Guadalajara, Mexico*, 161–166.
- Schügerl, K. and Bellgard, K.H. (2000). Bioreactor models. In K. Schügerl and K.H. Bellgard (eds.), *Bioreaction engineering: modelling and control*. Springer-Verlag Berlin Heidelberg.
- Tsuchiya, H.M., Fredrickson, A.G., and Aris, R. (1966). Dynamics of Microbial Cell Populations. *Advances in Chemical Engineering*, 6(C), 125–206.
- Villadsen, J. (1999). On the use of population balances. *J. Biotechnol.*, 71, 251–253.
- Waldherr, S. (2018). Estimation methods for heterogeneous cell population models in systems biology. *Journal of the Royal Society Interface*, 15(147).